Journal of Alloys and Compounds 491 (2010) 41–44

Contents lists available at ScienceDirect

Journal of Alloys and Compounds

journal homepage: www.elsevier.com/locate/jallcom

Magnetic structure of the quasi-two-dimensional compound $CoTa_2O_6$

E.J. Kinast[a], C.A. dos Santos[b], D. Schmitt[c], O. Isnard[d,*], M.A. Gusmão[b], J.B.M. da Cunha[b]

[a] Universidade Estadual do Rio Grande do Sul, Rua 7 de Setembro, 1156, 90010-191 Porto Alegre, Brazil
[b] Instituto de Física, Universidade Federal do Rio Grande do Sul, C.P. 15051, 91501-970 Porto Alegre, Brazil
[c] Laboratoire de Géophysique Interne et Tectonophysique, Université Joseph Fourier, B. P. 53, 38041 Grenoble Cedex 9, France
[d] Institut Néel, CNRS/Université Jospeh Fourier, avenue des martyrs B. P. 166, 38042 Grenoble Cedex 9, France

ARTICLE INFO

Article history:
Received 22 July 2009
Received in revised form 16 October 2009
Accepted 19 October 2009
Available online 5 November 2009

PACS:
64.75.+g
75.30.Kz
83.85.Hf

Keywords:
Two-dimensional magnetism
Trirutile
Neutron diffraction

ABSTRACT

We report on a detailed investigation of magnetic properties of $CoTa_2O_6$ using several techniques: neutron and X-ray diffraction, specific-heat, magnetic susceptibility, and magnetization measurements. The compound shows quasi-two-dimensional behavior due to its layered structure of alternating Co–O and Ta–O planes. We find that all magnetic moments lie entirely in the Co–O planes, along easy axes determined by the orientations of oxygen octahedra that surround the Co ions. The easy axes in successive magnetic planes have relative orientations that differ by 90°. Antiferromagnetic ordering is observed below 6.6 K, with propagation vectors (±1/4,1/4,1/4) associated to the two non-equivalent sets of Co^{2+} ions, whose magnetic moments are perpendicularly oriented.

1. Introduction

Trirutile compounds of the type $A_xA'_{1-x}B_2O_6$ (A, A' = Fe, Co, Ni; B = Ta, Nb, Sb) have been the subject of many investigations, due to their interesting structural and magnetic properties, with a rich variety of magnetic phases [1–12]. All the observed ordered phases can be classified as antiferromagnetic (AF), but they differ from a simple nearest-neighbor Néel ordering. For $Fe_xCo_{1-x}Ta_2O_6$ the magnetic phase of iron-rich samples ($x > 0.46$) is described by two propagation vectors, (1/2,0,1/2) and (0,1/2, 1/2), while that of cobalt-rich samples ($0 < x < 0.46$) is described by the vectors (±1/4,1/4,0), as determined from neutron-diffraction data [9]. Although pure $FeTa_2O_6$ presents the same magnetic structure of Fe-rich samples containing Co, the same does not happen in the opposite limit, as the compound $CoTa_2O_6$ shows yet another magnetic structure, which has been described as commensurate, with magnetic moments lying in the *ab* plane [9] or as a complex helical structure, with components in the basal plane as well as along the *c* direction [6].

With the aim of clarifying this issue, we report here a detailed experimental study of the magnetic properties of $CoTa_2O_6$, by means of neutron diffraction as well as magnetization, magnetic-susceptibility and specific-heat measurements.

$CoTa_2O_6$ crystallizes in the trirutile structure with space group $P4_2/mnm$. Co^{2+} ions occupy the corner (0,0,0) and center (1/2,1/2,1/2) of the tetragonal primitive unit cell. These two positions are non-equivalent because the O^{2-} octahedra that surround each Co have their in-plane principal axes rotated by 90° with respect to one another (see Fig. 1). Due to the tetragonal symmetry, these in-plane axes are shorter than the other ones, thus defining magnetic anisotropy axes with different orientations for corner and center Co spins. The Ta atoms are at positions (0,0,±z) and (1/2,1/2,±z) where z is close to 1/3. This yields a layered structure, with two Ta planes separating each pair of Co planes, favoring quasi-two-dimensional magnetic behavior.

In what follows, we present in detail our neutron-diffraction results and high-temperature magnetic measurements, discussing the observed magnetic structure of $CoTa_2O_6$ in the light of the low-dimensional anisotropic scenario described above.

2. Experimental and methods

Samples of $CoTa_2O_6$ were prepared and characterized as reported in Ref. [13].

Direct-current magnetization as a function of applied field, $M(H)$, was measured at the Institut Néel (CNRS/Université J. Fourier, Grenoble, France), using an extraction magnetometer [14]. The $M(H)$ curves were obtained with magnetic inductions up to 10 T, in the temperatures range 1.5–300 K. The magnetic susceptibility as a function of temperature, $\chi(T)$, was extracted from field-cooled magnetization data

* Corresponding author. Tel.: +33 4 76 88 11 46; fax: +33 4 76 88 10 38.
E-mail address: olivier.isnard@grenoble.cnrs.fr (O. Isnard).

0925-8388/$ – see front matter © 2009 Elsevier B.V. All rights reserved.
doi:10.1016/j.jallcom.2009.10.241

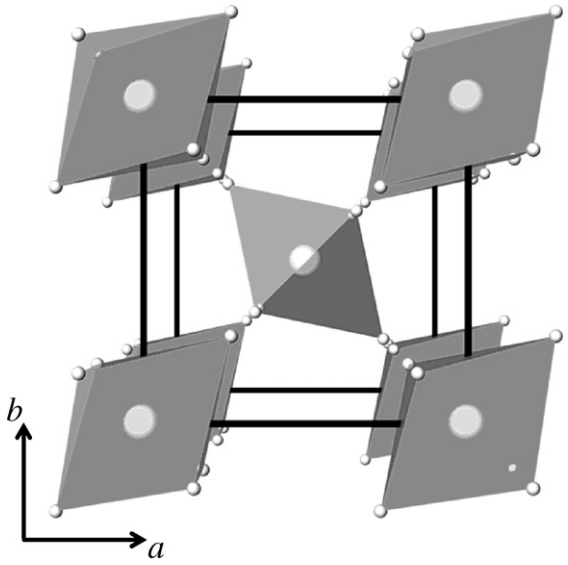

Fig. 1. Schematic representation of a unit cell of $CoTa_2O_6$, viewed along the c axis, showing three planes of Co ions and their surrounding oxygen octahedra. Large and small spheres represent Co and O atoms, respectively. For simplicity, Ta atoms have been omitted.

at a constant magnetic field $H = 5$ kOe, in the range 1.5–50 K. For temperatures above 50 K, up to room temperature, $\chi(T)$ was obtained by extrapolating the $M \times H$ data down to zero applied field, by means of the Arrott method [15].

In order to determine the magnetic transition temperature, specific-heat measurements were performed with an AC calorimeter [16], for temperatures ranging from 1.2 to 44 K.

Neutron diffraction measurements were performed on D1B, a powder diffractometer operated by the CNRS as a Collaborative Research Group at Institut Laue-Langevin (ILL), in Grenoble, France. Employing a wavelength of 2.52 Å, the angular position 2θ was varied from 5° to 85° with scan step of 0.2°. The diffractograms were taken at six temperatures: 1.5, 4, 5, 6, 9 and 12 K. Crystallographic and magnetic parameters were refined using the FullProf program [17].

3. Results and discussion

The magnetic susceptibility χ as a function of temperature is shown in Fig. 2. The Néel temperature is characterized by an inflection point at 6.6 ± 0.2 K, coinciding with the sharp peak observed in the specific-heat data, shown in Fig. 3. Above T_N, the χ vs T curve presents a broad maximum, indicating the presence of enhanced short-range correlations characteristic of low-dimensional materials. In the paramagnetic high-temperature region, we were able to fit the susceptibility data to a Curie–Weiss law, with Weiss constant $\theta_W = -29.6$ K, and effective magnetic moment $\mu_{\text{eff}} = 4.68\mu_B$ per

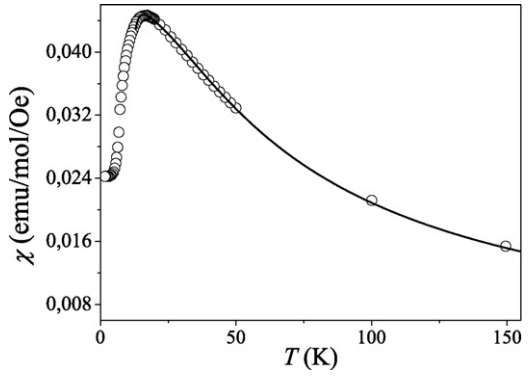

Fig. 2. Magnetic-susceptibility data of $CoTa_2O_6$ as a function of temperature (circles), and fitting via high-temperature series expansion (line).

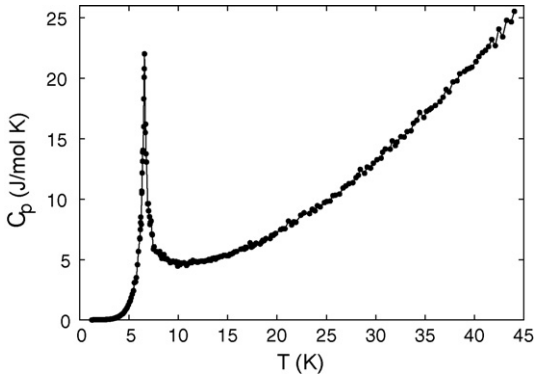

Fig. 3. Specific-heat data of $CoTa_2O_6$ as a function of temperature, showing a sharp peak at the magnetic transition.

Table 1
Best values of model parameters for a high-temperature series of the magnetic susceptibility.

J_1/k_B	−1.57 K
J_2/k_B	−1.96 K
D/k_B	18.31 K
$g_\parallel$	4.19 K
$g_\perp$	1.41 K

cobalt ion. This value of μ_{eff} is typical of high-spin Co^{2+} in octahedral geometry [18].

Going beyond the simple Curie–Weiss behavior, we fitted the susceptibility data to a high-temperature series expansion (continuous line in Fig. 2), using the anisotropic Heisenberg model on a square lattice proposed by Muraoka et al. [2] for $FeTa_2O_6$. We take $S = 3/2$ for the Co^{2+} spin, and adjust the remaining parameters of the model: a single-ion anisotropy coefficient D related to the in-plane easy axis mentioned above, the g-factor components along the anisotropy axis ($g_\parallel$) and transverse to it ($g_\perp$), and exchange constants J_1 and J_2, respectively for nearest neighbors and next-nearest neighbors on the square lattice. These two exchange interactions are comparable in magnitude due to the existence of superexchange paths involving two intermediate oxygen ions in both cases. Fitted values of the model parameters are listed in Table 1. Most important here is to notice the clear dominance of single-ion anisotropy, since D is much larger than the exchange constants, and $g_\parallel$ is substantially larger than $g_\perp$.

Table 2
Lattice constants, atomic positions, and magnetic moment obtained by Rietveld analysis of neutron-diffraction data at 12 and 1.5 K (respectively, first and second line in each case). Usual control parameters of the Rietveld method are included for the benefit of specialists (R_M = magnetic R-factor).

a (Å)	c (Å)	R_{wp} (%)	R_B (%)	R_M (%)
4.715(6)	9.128(0)	6.74	3.78	–
4.715(9)	9.127(6)	7.51	4.12	20.8

Atom	x	y	z	μ_{Co} (μ_B)
Co	0	0	0	–
	0	0	0	4.2(1)
Ta	0	0	0.32(9)	–
	0	0	0.32(9)	–
O1	0.31(2)	0.31(2)	0	–
	0.31(3)	0.31(3)	0	–
O2	0.297(0)	0.297(0)	0.32(4)	–
	0.296(8)	0.296(8)	0.32(3)	–

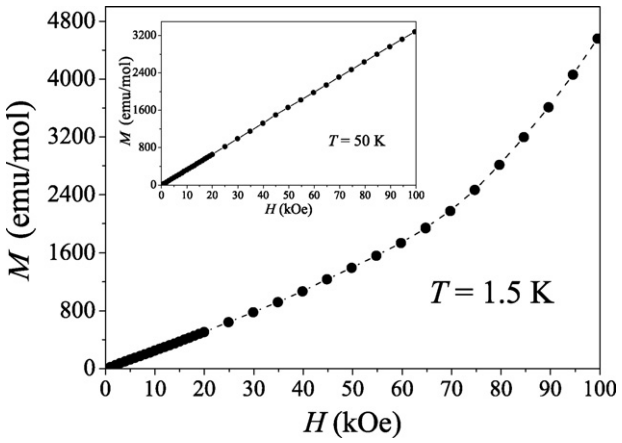

Fig. 4. Magnetization as a function of applied magnetic field for powder $CoTa_2O_6$ sample for $T < T_N$ (main plot) and $T > T_N$ (inset).

We want to point out that the same fitting was made in Ref. [9] for the entire series $Fe_xCo_{1-x}Ta_2O_6$. The anisotropy strength D shows an essentially linear variation with x, being highest for $CoTa_2O_6$ and lowest for $FeTa_2O_6$. In accordance to this, an X-ray analysis of the same system [13] indicated a linear reduction of the (positive) difference AO2 − AO1, these being the distances between a magnetic ion A and its nearest oxygen neighbors on the basal plane (O1) and out of it (O2). In other words, the in-plane octahedral axis is shortest when the anisotropy constant D is largest, which is consistent with our interpretation of this direction as the easy axis.

It is worth mentioning that simpler models have been employed to study magnetic properties of $CoTa_2O_6$, also emphasizing the low dimensionality and spin anisotropy. For instance, Kremer et al. [4] utilized a 2D Ising model to interpret specific-heat results.

An experimental signature of easy-axis magnetic anisotropy is a sudden change in the $M \times H$ curve at the field for which a spin-flop transition occurs. Indeed, this can be observed in Fig. 4 for magnetization curves recorded on powder sample. Although not as pronounced as one would have for a single-crystal sample [3], the low-temperature curve presents a clear change in slope around $H = 70$ kOe, in contrast to the linear behavior of the high-temperature plot shown in the inset. This relatively high critical field confirms that the anisotropy is strong. It is worth to notice that a critical field of similar magnitude has been reported for a single crystal of the isotype compound $FeTa_2O_6$[3].

We now turn to a neutron-diffraction analysis of the low-temperature magnetic structure. Fig. 5 shows our Rietveld-refined data obtained at 1.5 K. The solution was reached for a double-q ordering, with propagation vector (1/4,1/4,1/4) applied to the corner ions, their moments being aligned along the [1 1 0] direction, and (−1/4,1/4,1/4) for the center ions, with moments along the $[\bar{1}\,1\,0]$ direction. It can be seen that this configuration reproduces very well the angular positions of all the observed magnetic reflections.

For comparison, measurements were also performed at 12 K, i.e., above T_N. Characteristic parameters are listed in Table 2 for both temperatures. Cell constants and atomic positions are essentially unchanged, the only significant difference being the non-zero magnetic moment of cobalt seen only at the lower temperature. The atomic positions are consistent with our discussion of structural features in Section 1. As usual, only positions relative to the corner site are listed in Table 2; equivalent ones exist with respect to the central point at position (1/2,1/2,1/2).

The magnetic structure revealed by neutron diffraction can be described by a $2\sqrt{2}a \times 2\sqrt{2}a \times 4c$ primitive cell. For easier visualization, we use a larger conventional cell of dimensions $4a \times 4a \times 4c$, based on the original crystallographic axes. A schematic representation of the magnetic moments in such a cell is shown

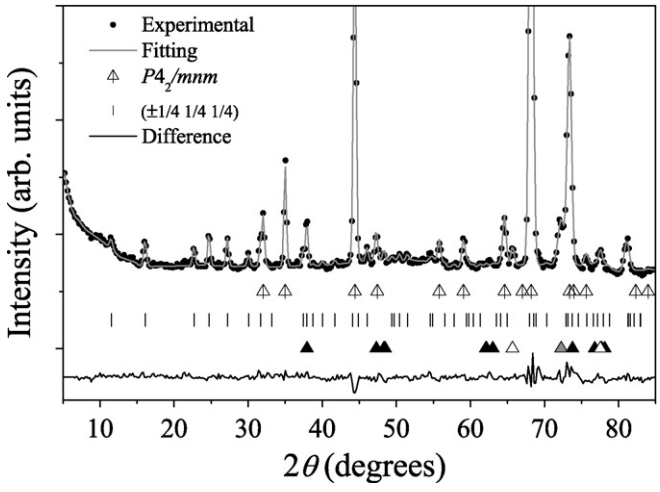

Fig. 5. Neutron diffraction pattern taken at 1.5 K, and Rietveld refinement. Besides the structure and magnetic reflections of $CoTa_2O_6$, we also see the signatures of small amounts of Ta_2O_5 (black triangles) and CoO (white triangles), as well as a vanadium reflection from the sample container (gray triangle).

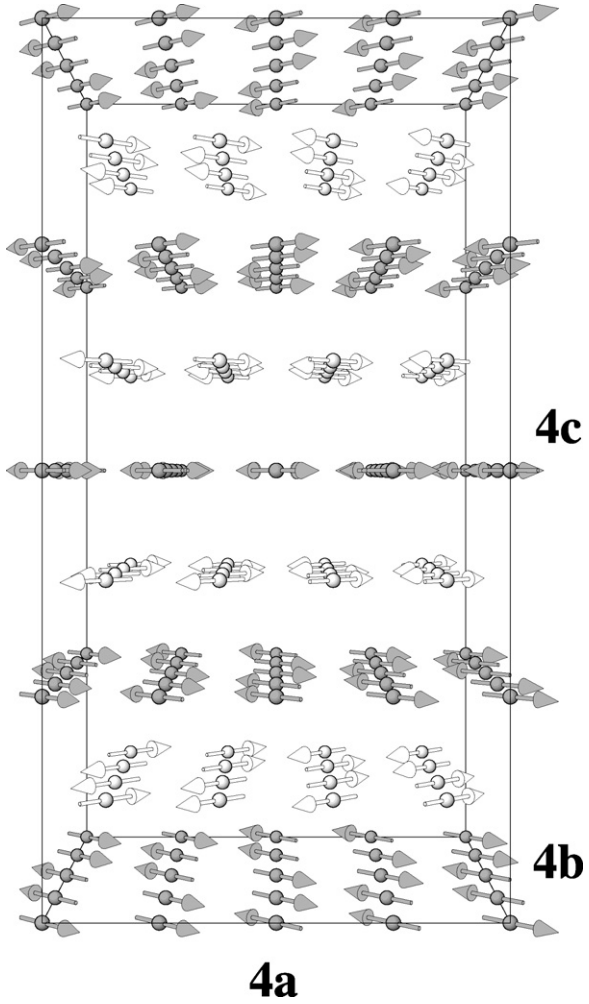

Fig. 6. Magnetic structure of Co moments as revealed by neutron-diffraction. Dark (bright) spheres represent corner (center) ions.

in Fig. 6. The moments are distributed as a sequence of the type "$++--++--$" along the three axes. In addition, the moments are rotated by 90° from one plane to the next, following the rotation of the anisotropy axis. Refining the neutron-diffraction data with the configuration of Fig. 6 reproduces well all the magnetic reflections, as seen in Fig. 5.

4. Conclusions

We have investigated the magnetic properties of $CoTa_2O_6$ with the aim of undoubtedly determining the nature of its low-temperature magnetic ordering, for which contrasting reports existed in the literature [9,6].

Our neutron-diffraction, susceptibility, and magnetization results clearly reveal the quasi-two-dimensional nature of magnetism in this compound, as well as the dominant role played by single-ion anisotropy. The latter finds its origin on the distorted geometry and spatial orientation of oxygen octahedra that surround the magnetic Co^{2+} ions. Based on these results, we provide strong evidence that the magnetically ordered phase has a spin structure as shown in Fig. 6, with a four-step repeating pattern along any of the tetragonal cell directions. It can be described by a pair of propagation vectors ($\pm$1/4,1/4,1/4), with all spins lying on the *ab* plane, and alternating their orientations between the [1 1 0] and [$\bar{1}$ 1 0] directions on successive planes. This result is in excellent agreement with the strong anisotropy resulting from the distortion of the octahedra surrounding the Co ions.

Similar patterns have been observed throughout the families of compounds $Fe_xCo_{1-x}Ta_2O_6$[9], and $Fe_xNi_{1-x}Ta_2O_6$[11,12], as well as for $CoSb_2O_6$[6], all sharing the common features of layered structure and single-ion anisotropy. Specific differences in spin arrangements observed in the various ordered phases can be attributed to the interlayer coupling that ultimately stabilizes three-dimensional ordering. This coupling being weak, as indicated by typical low values of Néel temperatures, should be strongly affected by composition changes. Such changes must cause distortions of the oxygen octahedra due to differences in magnetic-ion radii, yielding changes in length and angle of bonds involved in superexchange interactions. On the other hand, more dramatic effects are obtained with substitution of Nb for Ta, when the crystal structure changes to orthorhombic, and incommensurate magnetic phases appear [7].

The rich variety of magnetic behavior of AB_2O_6 compounds certainly deserves further investigation, preferably with emphasis on the role of interlayer coupling.

Acknowledgments

This work was supported in part by the Brazilian-France agreement CAPES-COFECUB and by the Brazilian agency CNPq.

References

[1] S.M. Eicher, J.E. Greedan, K.J. Lushington, J. Solid State Chem. (1986) 220.
[2] Y. Muraoka, T. Idogaki, N. Uryu, J. Phys. Soc. Jpn. 57 (1988) 1758.
[3] E.M.L. Ghung, M.R. Lees, G.J. McIntyre, C. Wilkinson, G. Balakrishnan, J.P. Hague, D. Visser, D.McK. Paul, J. Phys.: Condens. Matter 16 (2004) 7837.
[4] R.K. Kremer, J.E. Greedan, E. Gmelin, W. Daí, M.A. White, S.M. Eicher, K.J. Lushington, J. Phys. 49 (1988) 8–1495.
[5] J.P. Hague, E.M.L. Ghung, D. Visser, G. Balakrishnan, E. Clementyev, D.McK. Paul, M.R. Lees, J. Phys.: Condens. Matter 17 (2005) 7227.
[6] J.N. Reimers, J.E. Greedan, C.V. Stager, R.K. Kremer, J. Solid State Chem. 83 (1989) 20.
[7] C. Heid, H. Weitzel, F. Bourdarot, R. Calemczuk, T. Vogt, H. Fuess, J. Phys.: Condens. Matter 8 (1996) 10609.
[8] H. Ehrenberg, G. Wltschek, J. Rodriguez-Carvajal, T. Vogt, J. Magn. Magn. Matter 184 (1998) 111.
[9] E.J. Kinast, V. Antonietti, D. Schmitt, O. Isnard, J.B.M. da Cunha, M.A. Gusmão, C.A. dos Santos, Phys. Rev. Lett. 91 (2003) 19720.
[10] R.K. Kremer, J.E. Greedan, J. Solid State Chem. 73 (1988) 579.
[11] S.R. de Oliveira Neto, E.J. Kinast, M.A. Gusmão, C.A. dos Santos, O. Isnard, J.B.M. da Cunha, J. Phys.: Condens. Matter 19 (2007) 356210.
[12] S.R. de Oliveira Neto, E.J. Kinast, O. Isnard, J.B.M. da Cunha, M.A. Gusmão, C.A. dos Santos, J. Magn. Magn. Matter 320 (2008) E125.
[13] V. Antonietti, E.J. Kinast, L.I. Zawislak, J.B.M. da Cunha, C.A. dos Santos, J. Phys. Chem. Solids 62 (2001) 1239.
[14] A. Barlet, J.C. Genna, P. Lethuillier, Cryogenic 31 (1991) 801.
[15] A. Arrott, J.E. Noakes, Phys. Rev. Lett. 19 (1967) 786.
[16] M. Bouvier, P. Lethuillier, D. Schmitt, Phys. Rev. B 50 (1994) 13453.
[17] J. Rodriguez-Carvajal, Physica B 192 (1993) 55.
[18] D. Gignoux, M. Schlenker, in: E. du Trémolet de Lacheisserie (Ed.), Magnetism I: Fundamentals, Kluwer Academic Press, 2002.